Determination of liquid-liquid critical point composition using 90° laser light scattering

J. Charles Williamson,* Allison M. Brown, Elise N. Helvie, and Kevin M. Dean†
Department of Chemistry, Willamette University, 900 State Street, Salem, Oregon 97301, USA
(Received 7 August 2015; revised manuscript received 6 March 2016; published 21 April 2016)

Despite over a century of characterization efforts, liquid-liquid critical point compositions are difficult to identify with good accuracy. Reported values vary up to 10% for even well-studied systems. Here, a technique is presented for high-precision determination of the critical composition of a partially miscible binary liquid system. Ninety-degree laser light-scattering intensities from single-phase samples are analyzed using an equation derived from nonclassical power laws and the pseudospinodal approximation. Results are reported for four liquid-liquid systems (aniline + hexane, isobutyric acid + water, methanol + cyclohexane, and methanol + carbon disulfide). Compared to other methods, the 90° light-scattering approach has a strong dependence on composition near the critical point, is less affected by temperature fluctuations, and is insensitive to the presence of trace impurities in the samples. Critical compositions found with 90° light scattering are precise to the parts-per-thousand level and show long-term reproducibility.

DOI: 10.1103/PhysRevE.93.042610

I. INTRODUCTION

Characterization of liquid-liquid coexistence behavior is of both practical and fundamental importance. At the applied level, industrial and analytical separation techniques rely on detailed maps of phase behavior and solute partitioning. For example, current "green" solvent system candidates for chemical synthesis and extraction include binary liquid mixtures like ionic liquid + water and ionic liquid + organic [1–3]. Some of these mixtures exhibit partial miscibility and liquid-liquid critical behavior [4,5]. The critical temperature T_C and critical composition x_C in such solvent systems must be identified accurately, in part because reaction rates are altered in near-critical environments [6].

On the theoretical side, partially miscible binary liquid systems have been the vehicle for many investigations into critical point universality [7,8]. Nonclassical representations of critical phenomena continue to be refined [8–11], with additional considerations given to the impact of ionic components [5]. In keeping with longstanding practices [7], these theoretical models are assessed relative to measured liquid-liquid coexistence curves where the critical point must be known very well. For example, measurements of nitrobenzene + n-alkane systems were used to support the isomorphism principle and complete scaling theory [9–11], resolving the decades-old question [7] regarding the appropriate choice of order parameter for liquid-liquid systems.

Meticulous experimental standards must be observed in order to determine the value of x_C accurately for a liquid-liquid system. Constraints include maintenance of temperature control on the order of 1 mK and strict preservation of sample purity. Even with such efforts, accurate identification of x_C remains elusive. Data for the methanol + cyclohexane system illustrate the challenge: the methanol + cyclohexane system has been studied for over a century, but the critical compositions reported in 21 independent measurements range from 0.49 to 0.54 mole fraction methanol, a span of 10% (see Appendix A). In this manuscript we introduce a new laser light-scattering technique for determining x_C that we believe will lead to improved reproducibility between research groups.

In order to provide context for the advantages of our new method, we first discuss some limitations of using coexistence curve data to find x_C. In the synthetic method approach to liquid-liquid coexistence curve measurement, a suite of samples are prepared spanning the composition coordinate, and the coexistence temperature T_{cx} of each sample is measured [12]. The critical composition is often found by fitting the set of (x, T_{cx}) data to the simple scaling power-law equation for the coexistence curve [7,8]:

$$|x - x_C| = B_{cx}|t_{cx}|^{\beta}. \tag{1}$$

In Eq. (1), β is a universal critical exponent with an accepted value of 0.326 [13], B_{cx} is a system-specific amplitude, and t_{cx} is the reduced temperature:

$$t_{cx} = \frac{T_{cx} - T_C}{T_C}. \tag{2}$$

Using Eq. (1) to find x_C presents challenges. The basic analytical task is to identify a particular point on the independent variable axis (x_C) with high precision from measurements of the dependent variable (T_{cx}). In general, this task is best accomplished when the dependent variable changes rapidly in the vicinity of the target point, and less so further away from the point. Unfortunately, liquid-liquid coexistence curves exhibit the opposite mathematical behavior due to the fractional exponent β: liquid-liquid coexistence curves change very little with temperature in the vicinity of the critical point, and then change with increasing rapidity further from the critical point. As a result, when fitting coexistence curve data to Eq. (1) the data furthest from the critical point have the greatest influence on the value of x_C found with the fit. This is illustrated in Fig. 1. Figure 1(a) presents 14 coexistence curve data points we reported for the aniline + hexane system in an earlier publication [14]. The simple scaling equation (the dotted line) models the data well, and x_C can be found from the fit. To assess the robustness of the fit, Figure 1(b) presents a sample

*Corresponding author: jcwillia@willamette.edu
†Present address: Department of Cell Biology, The University of Texas Southwestern Medical Center, Dallas, Texas 75390, USA.

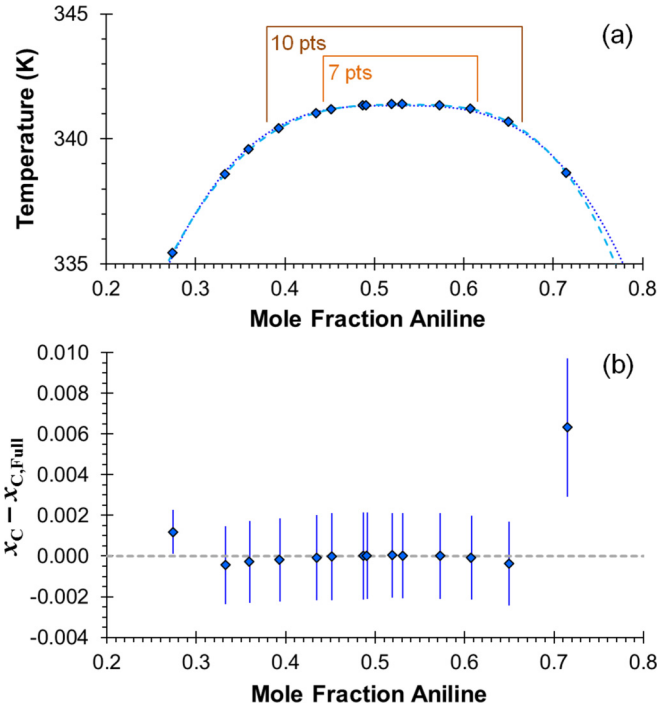

FIG. 1. (a) Aniline + hexane coexistence curve data from Ref. [14]. The data are fit with simple scaling [Eq. (1); dotted line] and truncated complete scaling [Eq. (3); dashed line]. (b) Sample removal test of the simple scaling fit. Error bars are 2 standard deviations as reported by the fitting software.

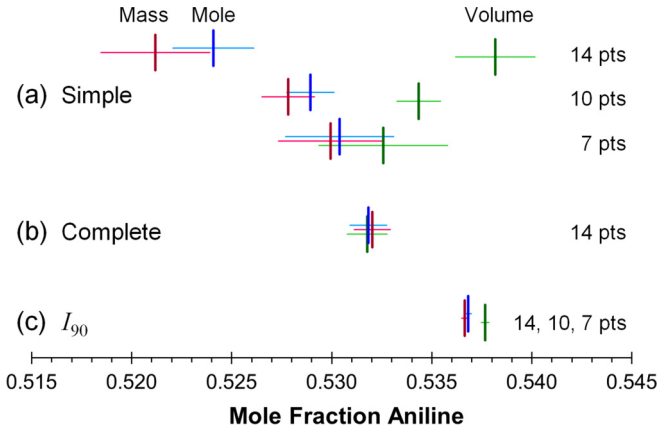

FIG. 2. Aniline + hexane critical composition determined using mole, mass, and volume fraction for the composition coordinate and using all 14 data points, 10 points, or 7 points. Horizontal bars indicate fitting uncertainty at 2 standard deviations. (a) Coexistence curve fit using simple scaling, Eq. (1). (b) Coexistence curve fit using complete scaling truncated at the D_2 term, Eq. (3). (c) 90° light-scattering fit using Eq. (20).

removal test on the data set. In this test, one of the 14 samples is removed from the data set and x_C is found by fitting the remaining data to Eq. (1). The test is done 14 times, once per sample, and the differences of each x_C relative to $x_{C,Full}$ (using all 14 data points) are plotted in Fig. 1(b) as a function of the composition of the sample that is removed. For example, Fig. 1(b) shows that the critical composition identified by the fit is +0.006 different if the sample at $x_{Ani} = 0.7148$ is not included, whereas the absence of a sample near x_C, such as $x_{Ani} = 0.5310$, has a negligible effect on the outcome of the fit. Since the outer points are the most influential, any asymmetry in the coexistence curve data, either intrinsic or extrinsically induced, may introduce systematic error into the determination of x_C.

One historical consequence of this dynamic is that the value found for x_C has been dependent on the choice of order parameter. Unless the molar masses and densities of the two pure components happen to be matched, the coexistence curve will have different degrees of asymmetry depending on whether the composition axis is expressed as mole fraction, mass fraction, or volume fraction. The wider the range of composition that is used in the fit, the greater the resulting disparity.

Figure 2(a) shows the values of x_C found when fitting Eq. (1) to the aniline + hexane data from Fig. 1(a) while using mole, mass, or volume fraction as the composition coordinate. The values of m_C and ϕ_C have been converted back to mole fractions in order to plot their locations on the graph; excess volume effects are negligible in this analysis. Figure 2(a) also shows how the span of the data affects the analysis. The data were first fit using all 14 points, and then again using the central 10 and 7 points [Fig. 1(a)]. The horizontal bars in Fig. 2(a) represent the uncertainty in x_C determined by the fitting software, reported here as 2 standard deviations. Varying the composition coordinate leads to three x_C values between 0.52 and 0.54 when using all 14 data points. These three values converge as the range of data used in the fit is narrowed, but then excellent experimental temperature stability becomes more and more important since the coexistence curve is so flat near x_C.

Some of these analysis issues are alleviated if the (x, T_{cx}) data are of sufficiently high quality to warrant fitting with higher-order expansions of the simple scaling equation, such as corrections to scaling [7], or the more recent complete scaling model [10,11]. Under the complete scaling model, the coexistence curve is described by:

$$\frac{x - x_C}{x_C} = \pm B_0 |t_{cx}|^{\beta} + D_2 |t_{cx}|^{2\beta} + D_1 |t_{cx}|^{1-\alpha} + D_0 |t_{cx}|, \tag{3}$$

where α is a universal critical exponent with a value of 0.110 [13]; B_0 is the coexistence curve amplitude; and D_0, D_1, and D_2 are leading coefficients on nonanalytic asymmetric terms. When our full aniline + hexane data set is fit with Eq. (3) truncated at the D_2 term [the dashed line in Fig. 1(a)], then the choice of composition coordinate no longer affects the value of x_C determined in the fit [Fig. 2(b)].

However, despite the excellence of the complete scaling fit to our aniline + hexane coexistence data, we will provide evidence in this paper that the x_C value found with Eq. (3) is still inaccurate. We suspect the inaccuracy is due to a trace third-component impurity in one of the starting components. Third-component impurities are well known to have a significant effect on measured T_{cx} values [7]. For example, trace water in the methanol + cyclohexane system increases T_C at a rate of 1 K per 0.1 mole percent water [15,16]. The presence of random impurities in synthetic method samples will randomize

the T_{cx} values, effectively defeating any attempts to achieve precise instrument temperature control while simultaneously degrading coexistence curve fitting efforts. Careful sample preparation techniques can avoid the problem of sample-to-sample impurity variation. However, the influence of systematic impurity effects is generally unappreciated. The presence of an impurity in just one of the starting components will make the coexistence curve asymmetric, and the maximum in the coexistence curve will not be at the critical point. Higher-order fits of the coexistence curve, such as Eq. (3), do not account for the effect of systematic third-component impurities and may yield erroneous values for x_C. Another approach is needed.

Here we present a 90° laser light-scattering technique for elucidating x_C that solves many of the problems described in the previous paragraphs. The 90° light-scattering signal has a much stronger composition dependence about the critical point than coexistence curve temperatures and is thus less dependent on the span of the data. At the same time, the 90° light-scattering signal is less sensitive to temperature variations near the critical point, so less-stringent temperature control is required. Most importantly, our method is remarkably insensitive to the presence of impurities in the samples.

In the following sections we present a development of the theoretical basis for our technique, and then assess its application to four liquid-liquid systems. We show that analysis of 90° laser light-scattering data yields highly reproducible x_C values with a precision equal to or better than other methods, and we propose that the results are more accurate as well.

II. THEORETICAL METHODS

Liquid-liquid mixtures scatter light strongly in the vicinity of the critical point due to enhancement of density and concentration fluctuations in the medium [17,18]. This light-scattering effect is known as critical opalescence, and we show here how opalescence is a sensitive quantitative probe for critical composition. Measurements of opalescence from critical and near-critical samples have been used to determine various universal critical exponents and amplitudes. Often the decline in transmitted light (the turbidity) is measured as $T \to T_C$. This approach requires great care in sample preparation in order to limit the occurrence of trace particulate Mie scattering, which is pronounced in the forward direction. Mie scattering is weak at larger scattering angles, at least for small particles and low number densities, but critical opalescence from the bulk solution is nearly isotropic. Therefore an experiment that relies on the collection of 90° light scattering has an advantage in that sample preparation requirements with respect to dust are less stringent. There is at least one report in which opalescence observed at 90° has been used to determine the critical composition of a ternary mixture, where x_C was not coincident with the extremum of the coexistence curve [19]. Here we present a formal derivation of how light-scattering intensity at 90°, I_{90}, depends on temperature and composition for a single-phase binary liquid system near the critical point. For simplicity, we present the derivation in terms of an upper critical point.

Along the critical isopleth, the scattering intensity I is proportional [17,20] to the susceptibility $\chi(q, T)$, where the scattering vector q is

$$q = 2k \sin\left(\frac{\theta}{2}\right). \tag{4}$$

In this equation, θ is the scattering angle, and the wave number k is related to the refractive index of the medium n and the vacuum wavelength of the light source λ_0:

$$k = \frac{2\pi n}{\lambda_0}. \tag{5}$$

The susceptibility $\chi(q, T)$ obeys a power law according to:

$$\chi(q,T) = \Gamma t^{-\gamma} g(q\xi), \tag{6}$$

where γ is a universal critical exponent with value 1.239 [13], Γ is the susceptibility amplitude, g is the correlation scaling function, and t is the reduced temperature $(T - T_C)/T_C$. The correlation length ξ in Eq. (6) also follows a power law:

$$\xi = \xi_0 t^{-\nu}. \tag{7}$$

Here ν is a universal critical exponent with value 0.630 [13], and ξ_0 is the correlation length amplitude.

In this derivation we use the Fisher correction to the Ornstein-Zernike correlation scaling function [18,20,21]:

$$g(q\xi) = \frac{1}{(1 + q^2\xi^2)^{1 - \eta/2}}. \tag{8}$$

The universal critical exponent η has the value 0.033 [13]. Combining Eqs. (4) and (6)–(8) leads to the following expression for the 90° light-scattering intensity:

$$I_{90,C}(T) \propto \frac{\Gamma t^{-\gamma}}{\left(1 + 2k^2\xi_0^2\, t^{-2\nu}\right)^{1 - \eta/2}}. \tag{9}$$

Incorporating the critical exponent relationship [13]:

$$\gamma = (2 - \eta)\nu, \tag{10}$$

will simplify Eq. (9) to:

$$I_{90,C}(T) \propto \frac{\Gamma}{\left(t^{2\nu} + 2k^2\xi_0^2\right)^{1 - \eta/2}}. \tag{11}$$

This equation describes the 90° light-scattering intensity as a function of temperature from a single-phase liquid-liquid sample at its critical composition.

Extension of Eq. (11) to off-critical compositions can be done by making the pseudospinodal approximation [22–24], where the susceptibility of a metastable single-phase sample continues to increase as the temperature drops past T_{cx} until the sample reaches a limit of stability analogous to the thermal spinodal curve [25]. Under the pseudospinodal approximation:

$$\chi(x,q,T) = \Gamma(x)(t^*)^{-\gamma^*} g(q\xi), \tag{12}$$

where the asterisk indicates a pseudospinodal critical exponent. Similarly, the correlation length is written as follows:

$$\xi(x) = \xi_0(x)(t^*)^{-\nu^*}. \tag{13}$$

Both Eq. (12) and Eq. (13) involve a reduced temperature t^* that is relative to the stability limit, the pseudospinodal

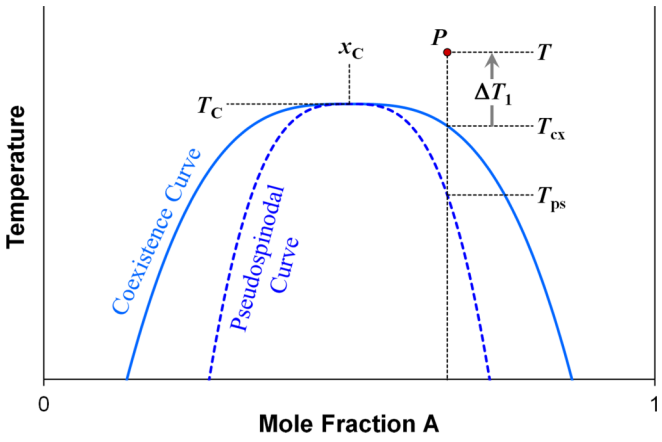

FIG. 3. Representative coexistence curve and pseudospinodal curve for a liquid-liquid system of components A and B.

boundary $T_{ps}(x)$:

$$t^* = \frac{T - T_{ps}(x)}{T_C}. \tag{14}$$

The pseudospinodal curve is assumed to have the same mathematical representation as the coexistence curve, but with a smaller amplitude. Following from Eq. (1), the pseudospinodal curve is defined by:

$$|x - x_C| = B_{ps}\left|\frac{T_{ps} - T_C}{T_C}\right|^{\beta^*}. \tag{15}$$

Figure 3 shows the relationship between the coexistence curve and the pseudospinodal curve.

Data on the composition dependences of critical amplitudes and pseudospinodal critical exponents are limited. Fusenig and Woermann found that there was no composition dependence for ξ_0 in the 2-butoxyethanol + water system, and that the pseudospinodal exponents ν^* and γ^* were very similar to their critical counterparts [22]. The authors observed a decrease in the susceptibility amplitude $\Gamma(x)$ on the order of 25% as composition moved away from the critical composition. In contrast, Lesemann *et al.* found composition dependencies for all four of these parameters in a system involving heavy water and aggregating nonionic surfactants [26]. Given that the liquid-liquid systems we are describing are small-molecule systems, we follow the findings of Fusenig and Woermann by treating ξ_0 and Γ as system constants, and we assume that $\nu^* = \nu$ and $\gamma^* = \gamma$ are universal relationships.

A number of experiments have been carried out to determine β^*, and the general conclusion is that $\beta^* = \beta$, with the possibility that β^* is slightly larger [27–30]. There are also experimental and theoretical reports that the amplitude ratio B_{ps}/B_{cx} is a constant on the order of 0.63 [27,28,30]. In the derivation here it is assumed that $\beta^* = \beta$, but the amplitude ratio is not constrained.

Following from the pseudospinodal approximation and the preceding assumptions, the temperature and composition dependence of the 90° scattering intensity can be adapted from Eq. (11) by replacing t with t^*:

$$I_{90}(x,T) = \frac{C}{\left[(t^*)^{2\nu} + 2k^2\xi_0^2\right]^{1-\eta/2}}. \tag{16}$$

The proportionality constant C incorporates the susceptibility amplitude Γ, and the composition dependence of I_{90} comes in through $T_{ps}(x)$ in t^* [Eq. (14)]. Equation (16) may be used without direct measurement of $T_{ps}(x)$ by carrying out the following steps. In our synthetic method experiments we measure I_{90} as a function of temperature in the single-phase region, and we determine T_{cx} for each sample composition. If the sample is at some point ***P*** in the single-phase region (Fig. 3), then we define ΔT_1 as the difference between the sample's temperature T and its coexistence curve temperature T_{cx}. The expression for t^* [Eq. (14)] is then rewritten in terms of ΔT_1:

$$t^* = \frac{\Delta T_1 + T_{cx}(x) - T_{ps}(x)}{T_C}. \tag{17}$$

By solving Eqs. (1) and (15) for T_{cx} and T_{ps}, respectively, the difference between coexistence curve temperature and pseudospinodal temperature can be expressed as:

$$T_{cx} - T_{ps} = T_C \Delta B' |x - x_C|^{1/\beta}, \tag{18}$$

where $\Delta B'$ is defined as:

$$\Delta B' = B_{ps}^{-1/\beta} - B_{cx}^{-1/\beta}. \tag{19}$$

Substituting Eqs. (17) and (18) into Eq. (16) gives our target expression for 90° light-scattering intensity as a function of composition and temperature:

$$I_{90}(x,\Delta T_1) = \frac{C}{\left[\left(\frac{\Delta T_1}{T_C} + \Delta B' |x - x_C|^{1/\beta}\right)^{2\nu} + 2k^2\xi_0^2\right]^{1-\eta/2}}. \tag{20}$$

III. EXPERIMENTAL METHODS

A. Sample preparation

Preparations of the aniline + hexane, isobutyric acid + water, and methanol + cyclohexane samples have been described elsewhere [14,31]. Methanol + carbon disulfide (MCS) mixtures were created using starting components purchased from Aldrich with 99.99% purity specifications. MCS samples were prepared on a vacuum line by sequentially trapping vapor from the two starting components in liquid-nitrogen-cooled custom 14-mm OD glass ampules. Each 2.5-mL ampule contained a Teflon-coated spin bar. Ampules were flame-sealed after sufficient methanol and carbon disulfide had been transferred. The composition of each MCS ampule was determined gravimetrically, and corrections were made for buoyancy and for the moles of vapor occupying the head space in the sealed ampule.

B. Light-scattering measurements

Our methods of data collection have been described previously [14,31]. Briefly, the T_{cx} of each sample was determined to within 0.01 K using a stir-settle laser light-scattering technique. Transmitted light, small-angle scattering, and 90° scattering with s-polarization geometry were collected

simultaneously as a function of temperature out to ΔT_1 on the order of 0.5 K. To mitigate the effects of multiple scattering and self-attenuation in highly opalescent samples, 90° light scattering was collected from only the initial 2–6 mm of the laser's passage through the ampules. Tests showed that the value of x_C found from fitting I_{90} data was independent of optical path length over this range of distance.

To collect the I_{90} data, samples were taken from the single-phase region into the two-phase region and back in a sequence of 0.01 K temperature steps. Each run took approximately 1 day to complete, ensuring that samples had several minutes to equilibrate after every step. Data collected while decreasing the temperature were consistent with data collected while increasing the temperature: no hysteresis was observed. Nearly all samples have exhibited long-term stability, with T_{cx} values drifting by only a few hundredths of a kelvin over years of storage.

C. Data analysis

Assignment of T_{cx} for each sample was based on changes in the three light signals [31]. Values of T_{cx} from the scans of decreasing and increasing temperature almost always agreed to within 0.01 K and were averaged together. Coexistence curve data were fit to Eqs. (1) or (3) using the program PEAKFIT (Systat Software). The I_{90} data from all samples were compiled into a single table. To determine x_C with Eq. (20), the compiled I_{90} surface data were then fit as a function of x and ΔT_1 using the program TABLECURVE 3D (Systat Software). Our fits typically had five parameters: x_C, $\Delta B'$, $2k^2\xi_0^2$, the proportionality constant C, and a constant baseline offset for I_{90}. We used literature values for the critical exponents [13], and T_C was determined independently from the coexistence curve data. An initial four-parameter fit was done with a zero baseline. The baseline value was assigned by examining the fitting residuals for those samples well removed from the critical composition. The data were then refit using the new baseline offset as a fixed parameter.

IV. RESULTS AND DISCUSSION

A. Evaluation of the I_{90} approach

Results from measurements of the aniline + hexane system illustrate many of the advantages of using I_{90} data to find the liquid-liquid critical composition. The aniline + hexane samples were prepared a decade ago, but the data shown here were recollected from the samples 6 years later once our experimental techniques had been refined. Figure 4 shows (x_{Ani}, ΔT_1, I_{90}) data for the system, along with the corresponding surface fit to Eq. (20). As with all of the 90° light-scattering data for our liquid-liquid systems, Eq. (20) describes the aniline + hexane I_{90} data very well.

To demonstrate that the I_{90} data are more sensitive to the location of the critical composition than T_{cx} data, Fig. 5(a) juxtaposes the aniline + hexane coexistence curve with a slice of the I_{90} surface at $\Delta T_1 = 0.05$ K. The fit of Eq. (20) through this ΔT_1 slice is also shown. When the width of the coexistence curve is 0.100 on the mole fraction axis, the coexistence curve temperature has decreased below T_C by only 0.04 K. However, the I_{90} data have decreased to 45% of their maximum value

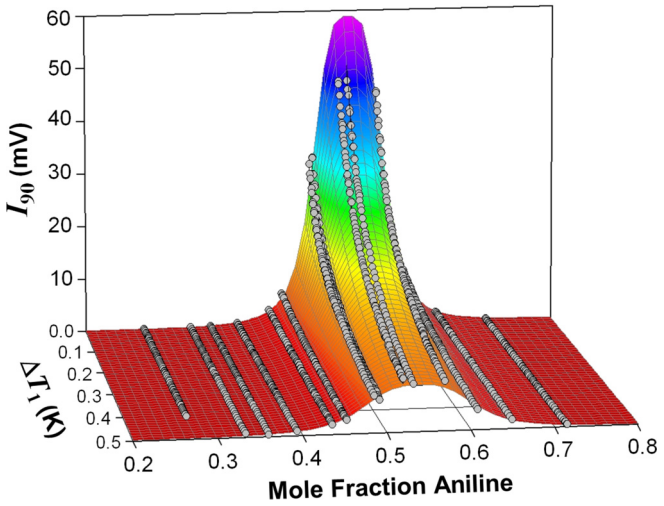

FIG. 4. Three-dimensional plot of I_{90} data for the aniline + hexane system with an overlay of the corresponding surface fit to Eq. (20). The I_{90} data were collected 6 years after the samples were prepared.

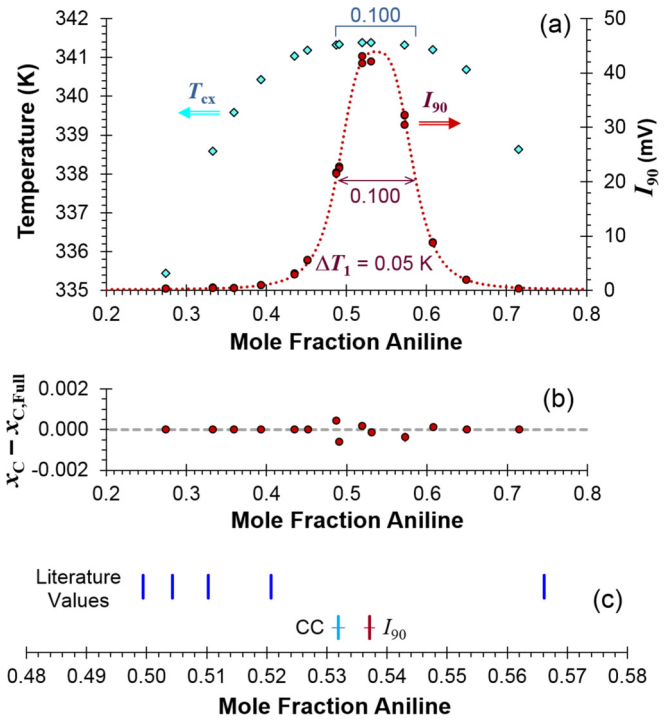

FIG. 5. (a) Initial coexistence curve data for the aniline + hexane system (light blue diamonds) compared against the corresponding I_{90} data for $\Delta T_1 = 0.05$ K (dark red circles). The I_{90} data were collected 6 years after sample preparation. The red dashed line is from the surface fit of the I_{90} data to Eq. (20). (b) Sample removal test of the I_{90} data fit. Error bars, barely visible, are 2 standard deviations as reported by the fitting software. (c) Comparison between literature values of the aniline + hexane critical composition (dark blue lines) with the measurement reported here. The light blue line is from a truncated complete scaling fit of the initial coexistence curve (CC); the red line is from analysis of I_{90} data collected 6 years later. Literature references are found in Appendix B.

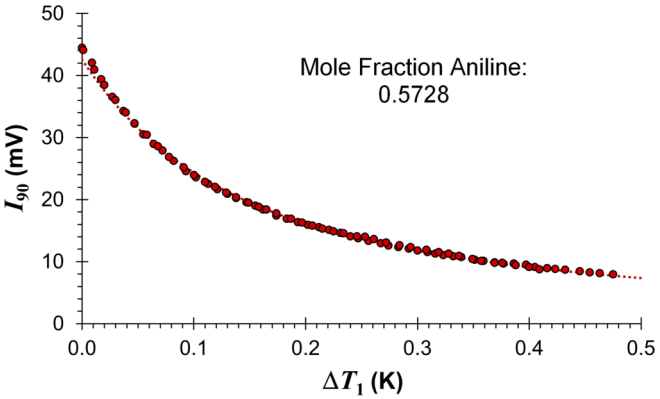

FIG. 6. Aniline + hexane I_{90} data versus ΔT_1 for a sample with an aniline mole fraction of 0.5728. The red dashed line is from the surface fit of the I_{90} data to Eq. (20). The I_{90} data were collected 6 years after sample preparation.

at x_C over this same composition span. Therefore, the most important samples for identifying x_C with I_{90} data are samples near x_C. This idea is confirmed in Fig. 5(b), a sample removal test using the I_{90} data. The results of the fit are perturbed only when a sample near x_C is removed from the full data set. Figure 5(b) should be compared with Fig. 1(b), the sample removal test based on coexistence curve data. In Fig. 1(b), the samples furthest from x_C have the greatest influence on the value of x_C found in the fit.

While good temperature control is certainly important for critical composition measurements based on I_{90} data, the experimental demands are not as strenuous as when the critical composition is determined from T_{cx} data. Figure 6 shows I_{90} data as a function of ΔT_1 for an aniline + hexane sample near the critical composition. At its steepest point near $\Delta T_1 = 0$, an 0.01 K fluctuation in temperature results in an I_{90} signal fluctuation on the order of a few percentages. In contrast, the coexistence curve at the same composition has dropped only 0.02 K below the critical temperature. A 0.01 K fluctuation in temperature corresponds to half of the signal that is being measured, $T_{cx} - T_C$, for determination of the critical composition with either the simple or complete scaling equations [Eqs. (1) and (3)].

Use of I_{90} data to find x_C is also less sensitive to the choice of composition coordinate, even though Eq. (20) is based on simple scaling equations. This is because the outcome of the fit is most influenced by those samples close to x_C. Earlier in Fig. 2(a) it was shown how the choice of the order parameter and the span of the data affected the outcome of fitting a coexistence curve with the simple scaling equation [Eq. (1)]. Figure 2(c) is a repeat of these tests using I_{90} data, and there are three key differences. First, the choice of composition coordinate has only a small effect on the outcome: the resulting three critical compositions (x_C, m_C, and ϕ_C) are clustered within 0.001 mole fraction aniline of one another. Second, the choice of the span of the data has no effect on the outcome of the fit. The central seven points all have I_{90} signals that are at least 10% of the I_{90} peak maximum [Fig. 5(a)]; sample removal tests show that points below the 10% threshold have little impact on the outcome of the fit, aside from helping to establish the baseline of the I_{90} data. Third, the uncertainty in x_C found in the fitting software's statistical report is typically at least an order of magnitude smaller with I_{90} data than with coexistence curve data.

Figure 5(c) compares our measured critical composition for the aniline + hexane system with five values found in the literature (see Appendix B). Since Eq. (20) is based on simple scaling theory, we report a x_C value that is an average of the three x_C values obtained when using mole, mass, and volume fraction as composition coordinates. Averaging these three values is qualitatively consistent with how the critical compositions are observed to converge [Fig. 2(a)] when using coexistence curve data and the simple scaling equation [Eq. (1)]. In future work we intend to incorporate complete scaling theory into Eq. (2), and we anticipate that the three x_C values will become even more tightly clustered.

The uncertainty we report for x_C combines together three quantities: the uncertainty in x_C reported by the fitting software; the standard deviation of the three x_C values found using mole, mass, and volume fraction; and the maximum deviation in x_C observed in the sample removal tests. Figure 5(c) shows our results for both I_{90} data analysis [Fig. 2(c)] and the fit of the truncated complete scaling equation to the coexistence curve data [Fig. 2(b)].

Coupled with our sample preparation techniques, the I_{90} analysis method yields critical composition values that are reproducible over many years. We have carried out long-term tests on the isobutyric acid + water and methanol + cyclohexane systems. Two separate sets of isobutyric acid + water samples were tested independently. First, Fig. 7(a) shows the coexistence curve initially measured for 25 isobutyric acid + water samples (Set A), along with a slice of the I_{90} surface at $\Delta T_1 = 0.05$ K collected 2 years later. Figure 7(b) shows the corresponding sample removal test for the I_{90} measurements. In the past, volume fraction [32] and mass fraction [33] were both recommended for the isobutyric acid + water composition coordinate because the coexistence curve is substantially more symmetric under these coordinates than with mole fraction. We observe slight but distinct asymmetry when the I_{90} data are plotted using the mole fraction coordinate. Since our I_{90} equation is based on simple scaling theory and does not yet account for higher-order terms found in Eq. (3), we present isobutyric acid + water data here with respect to the mass fraction coordinate. Volume fraction results are very similar to mass fraction, differing by only 0.0001 when converted back to the mass fraction coordinate.

Light-scattering measurements on Set A were repeated 7 and 10 years after the samples were prepared, and the resulting m_C values are compared in Fig. 7(c). The variation in m_C over the time span of observation is 0.0015 mass fraction isobutyric acid. For confirmation, we prepared a second set of isobutyric acid + water samples from new starting materials (Set B), and the critical composition we initially determined from that set of samples is consistent with Set A. Figure 7(c) also compares our results to 12 other independent measurements of the isobutyric acid + water critical composition (see Appendix C).

The second system we tested for long-term reproducibility was a smaller set of nine methanol + cyclohexane liquid-liquid samples. Figure 8 shows the initial coexistence curve, a slice of the I_{90} surface at $\Delta T_1 = 0.05$ K collected 5 years after sample preparation, and the sample removal test.

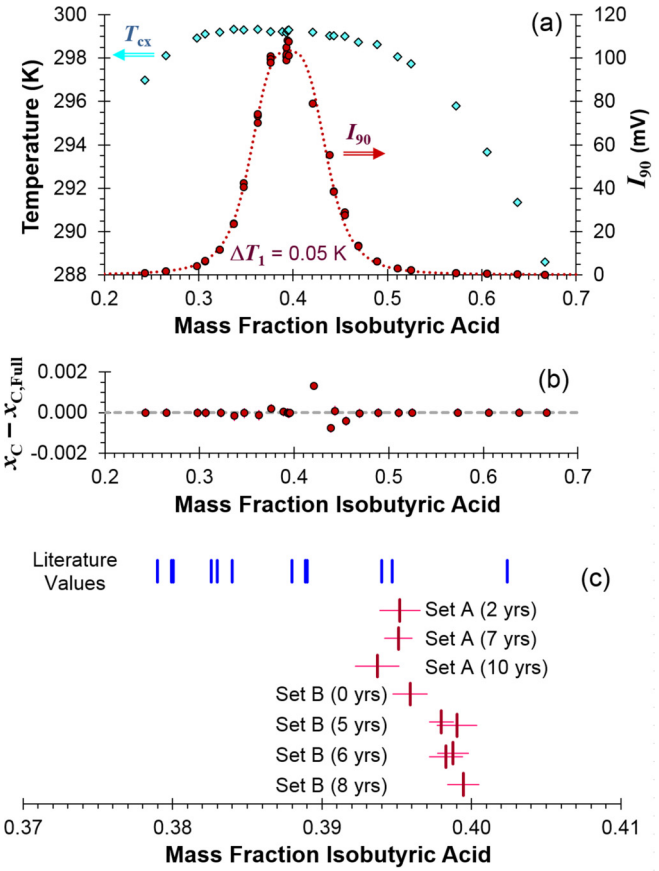

FIG. 7. (a) Initial coexistence curve data for Set A of the isobutyric acid + water system (light blue diamonds) compared against the corresponding I_{90} data for $\Delta T_1 = 0.05$ K (dark red circles). The I_{90} data were collected 2 years after sample preparation. The red dashed line is from the surface fit of the I_{90} data to Eq. (20). (b) Sample removal test of the I_{90} data fit. Error bars, barely visible, are two standard deviations as reported by the fitting software. (c) Comparison between literature values of the isobutyric acid + water critical composition (blue lines) with the two sets of measurements reported here using I_{90} data (red lines). The samples in Set B were incubated after initial measurements were made, leading to long-term changes in T_{cx} values—see the text. Literature references are found in Appendix C.

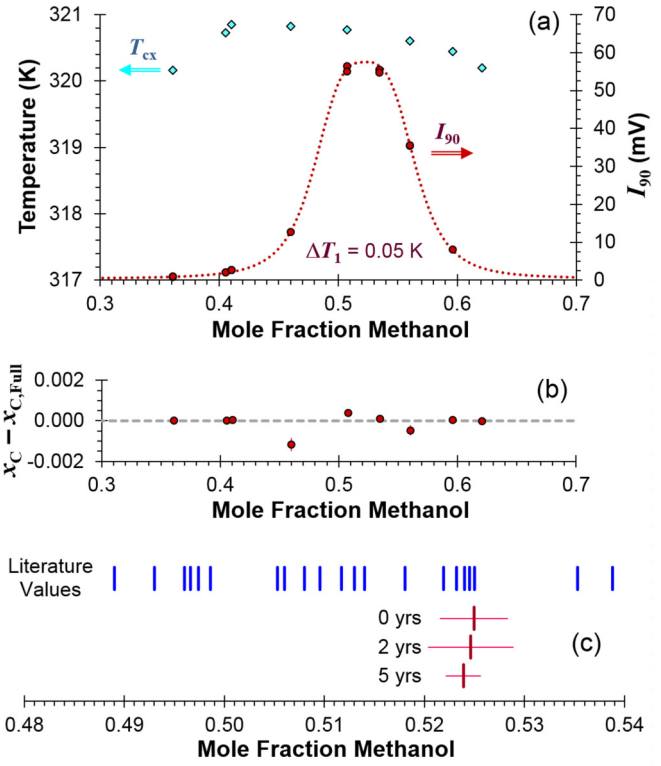

FIG. 8. (a) Initial coexistence curve data for the methanol + cyclohexane system (light blue diamonds) compared against the corresponding I_{90} data for $\Delta T_1 = 0.05$ K (dark red circles). The I_{90} data were collected 5 years later. The red dashed line is from the surface fit of the I_{90} data to Eq. (20). (b) Sample removal test of the I_{90} data fit. Error bars, just visible, are 2 standard deviations as reported by the fitting software. (c) Comparison between literature values of the methanol + cyclohexane critical composition (blue lines) with the measurements reported here using I_{90} data (red lines). Literature references are found in Appendix A.

Also shown are methanol + cyclohexane critical composition values found from the initial I_{90} measurements and from I_{90} measurements 2 and 5 years later. The critical composition is reproducible to within 0.001 mole fraction methanol over the 5-year span. Figure 8(c) compares our observations against the aforementioned 21 independent measurements of x_C for the methanol + cyclohexane system listed in Appendix A.

B. Impurity effects

Perhaps the most important benefit of using I_{90} data in a synthetic method determination of critical composition is that sample impurities have a very small effect on the analysis. While an impurity can significantly change coexistence curve temperatures for a liquid-liquid system, the critical composition undergoes a comparatively minor shift. Jacobs has characterized the effect of an impurity on critical point location in a liquid-liquid system by a simple empirical relationship [34]:

$$\left|\frac{x_C - x_{C,0}}{x_{C,0}}\right| = f\left|\frac{T_C - T_{C,0}}{T_{C,0}}\right|. \tag{21}$$

Here $x_{C,0}$ and $T_{C,0}$ define the critical point location in the absence of the impurity, and f is a proportionality constant on the order of 1. If an impurity causes a 1 K shift in the critical temperature of a liquid-liquid system with $T_{C,0} = 300$ K and $x_{C,0} = 0.5$, then Eq. (21) predicts that the critical composition will shift by 0.0017.

As an example, our values of x_C for the methanol + cyclohexane system may be a little high. Although our samples were prepared carefully under anhydrous conditions, we measured a coexistence curve with a critical temperature about 2 K above the recommended value [35]. An elevated T_C often indicates the presence of water in one or both of the original components. If, in fact, trace water was present in the set of methanol + cyclohexane samples we prepared, then the critical composition would be expected to be 0.002 to 0.003 lower [15,16] in mole fraction of methanol. Still, this potential disparity in x_C is much smaller in magnitude than the

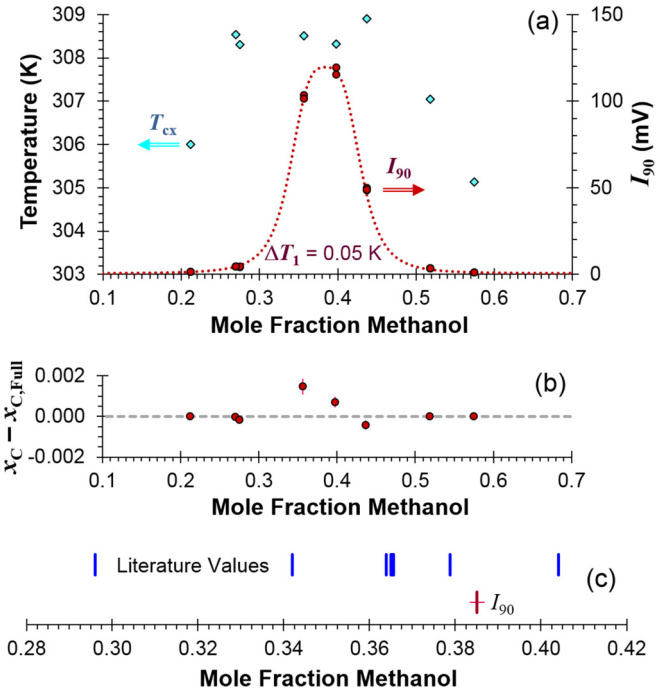

FIG. 9. (a) Initial coexistence curve data for the methanol + carbon disulfide system (light blue diamonds) compared against the corresponding I_{90} data for $\Delta T_1 = 0.05$ K (dark red circles). The I_{90} data were collected 7 years after sample preparation. The red dashed line is from the surface fit of the I_{90} data to Eq. (20). (b) Sample removal test of the I_{90} data fit. Error bars, just visible, are 2 standard deviations as reported by the fitting software. (c) Comparison between literature values of the methanol + carbon disulfide critical composition (blue lines) with the measurement reported here using I_{90} data (red line). Literature references are found in Appendix D.

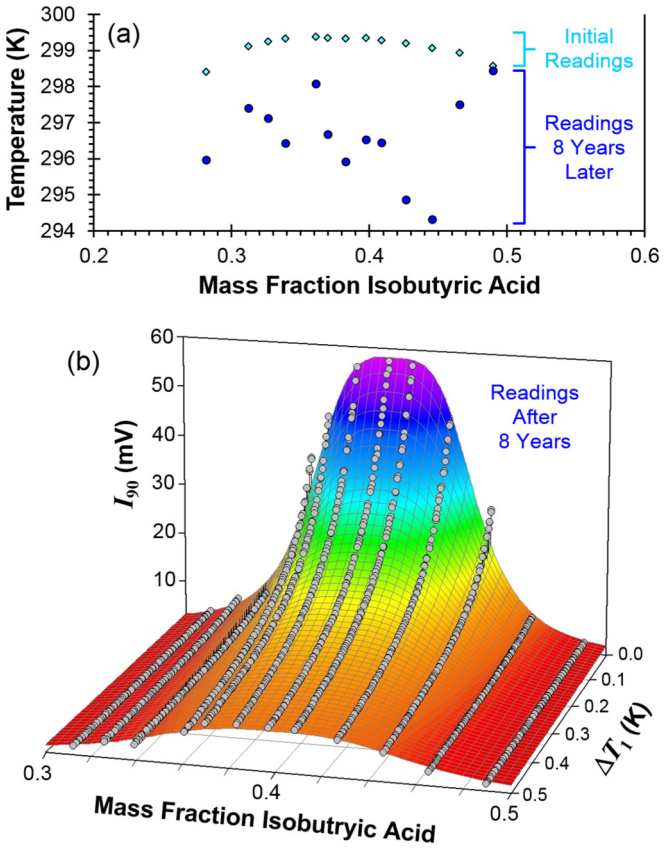

FIG. 10. (a) Initial coexistence curve data for Set B of the isobutyric acid + water system immediately after sample preparation (light blue diamonds) and 8 years later (dark blue circles). The Set B samples were incubated for 2 months at 35 °C shortly after the initial measurements. (b) Three-dimensional plot of I_{90} data at 8 years, and the corresponding surface fit to Eq. (20).

variation already observed in literature values for the methanol + cyclohexane system [Fig. 8(c)].

More generally, the presence of either systematic or random sample impurities readily compromises coexistence curve fits to Eqs. (1) and (3). This is seen in our methanol + cyclohexane coexistence curve, where the maximum of the curve does not line up with the I_{90} peak or even with the span of literature values for x_C. In contrast, I_{90} data are weakly dependent on the presence of impurities. According to Eq. (20), the I_{90} data depend on ΔT_1, the temperature *relative* to T_{cx}; the data do not depend on the specific values of T_{cx}. In other words, introduction of an impurity shifts the temperature dependence of the I_{90} data along with T_{cx}. The I_{90} data are only slightly affected by the accompanying small change in x_C.

We tested this prediction with experiments on two liquid-liquid systems. First, Fig. 9(a) shows the initial coexistence curve for a small set of methanol + carbon disulfide samples. The quality of the coexistence curve data in this case was substandard because the eight samples were prepared at different times over a one-month window rather than in a single session. Prolonged sample preparation opens up the possibility for introducing different types and amounts of impurities into each sample, leading to variations in T_{cx} such as those seen in Fig. 9(a). However, the corresponding slice of I_{90} data collected 7 years later [Fig. 9(a)] does not exhibit the same type of error and follows closely the model of Eq. (20). The sample removal test in Fig. 9(b) shows that x_C is well defined even though there are only three samples with I_{90} scattering intensities that are at least 10% of the peak maximum. Figure 9(c) compares our results with values reported in the literature (see Appendix D).

Even stronger evidence for the robustness of I_{90} data analysis with respect to impurities is presented in Fig. 10. After the isobutyric acid + water samples in Set B were first measured, the samples were incubated at 35 °C for 2 months. The T_{cx} values have dropped continuously over time since then, indicating that the incubation initiated some type of sample degradation process. Each sample has changed at a different rate, and Fig. 10(a) shows the T_{cx} values we measured 8 years later. The decreases in T_{cx} relative to the initial observations range from 0.1 K to 5 K, with an average drop of 2.5 K across the 13 isobutyric acid + water samples.

The resulting "coexistence curve" at 8 years [Fig. 10(a)] is impossible to evaluate for m_C using Eq. (1) or Eq. (3). However, the degradation products have only a small effect on the individual light-scattering properties of each sample, and the change is systematic. Figure 10(b) presents the I_{90} surface plot generated from a measurement of these samples at 8 years. The I_{90} data remain self-consistent in a way not at all suggested

by the T_{cx} data, and the resulting value of m_C has the same level of uncertainty as the measurement taken when the samples were first prepared. The value of m_C at 8 years is 0.0036 larger in mass fraction isobutyric acid relative to the initial measurement [Fig. 7(c)]. A shift of this magnitude is consistent with the observed average 2.5 K drop in T_{cx} [Eq. (21)].

V. SUMMARY AND CONCLUSIONS

The variability seen in literature reports for critical compositions of liquid-liquid systems can be attributed to three interrelated factors: the span of the data along the composition axis, the choice of composition coordinate, and the effect of impurities. We have developed a 90° laser light-scattering technique that mitigates all of these factors, and we have tested our method on four liquid-liquid systems: aniline + hexane, isobutyric acid + water, methanol + cyclohexane, and methanol + carbon disulfide. Our method shows long-term reproducibility and affords a precision of at least 0.001 mole fraction.

Table I presents a summary of our measurements. For each system we list the year of sample preparation, the number of samples in the set, the number of samples with I_{90} signals that are at least ten percent of the peak maximum, the year of I_{90} data collection, and the resulting critical composition. Critical composition uncertainties are based on sample removal tests, varying the composition coordinate, and statistical output from the fitting software.

An interesting question arises when our results for the aniline + hexane system are evaluated closely: Why is there a significant difference between the critical compositions found with complete scaling theory versus I_{90} data analysis [Figs. 2(b) and 2(c)]? Applying truncated Eq. (3) to the aniline + hexane coexistence curve (Fig. 1) yields a $x_{C,Ani}$ of 0.5318 ± 0.0010 when using the mole fraction composition coordinate. Applying Eq. (20) to the I_{90} data collected 6 years

TABLE I. Liquid-liquid critical compositions measured with 90° laser light scattering.

Set	Number of samples (# $I_{90} \geqslant 10\%$)	Years since sample preparation	Critical composition from I_{90} data
Aniline + Hexane			Mole Frac. Aniline
	14 (7)	6	0.5370 ± 0.0008
Methanol + Cyclohexane			Mole Frac. Meth.[a]
	9 (5)	0	0.525 ± 0.003
		2	0.525 ± 0.004
		5	0.5239 ± 0.0017
Methanol + Carbon Disulfide			Mole Frac. Meth.
	8 (3)	7	0.3851 ± 0.0017
Isobutyric Acid + Water			Mass Frac. IBA
A	25 (14)	2	0.3952 ± 0.0013
		7	0.3951 ± 0.0009
		10	0.3937 ± 0.0015
B	13 (10)	0	0.3959 ± 0.0011
		5[b]	0.3980 ± 0.0008
		5[b]	0.3990 ± 0.0013
		6[b]	0.3988 ± 0.0010
		6[b]	0.3983 ± 0.0011
		8[b]	0.3994 ± 0.0010

[a]Values may be elevated by 0.002–0.003 due to impurities. See text.
[b]Samples were incubated at 35 °C for 2 months after initial readings. See text.

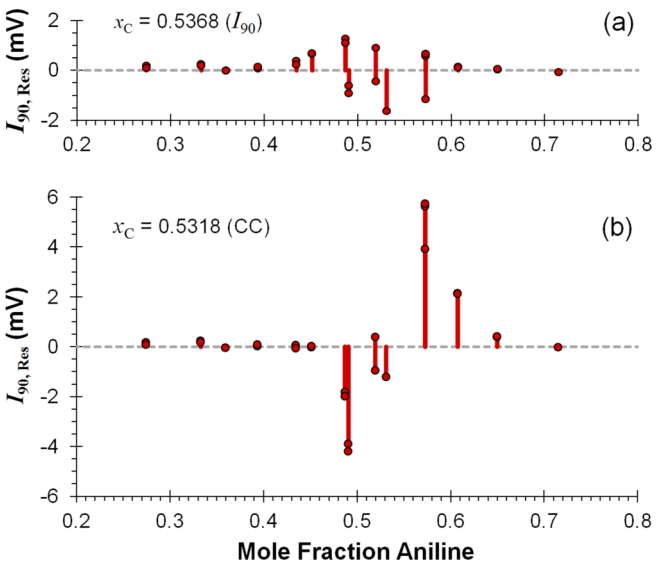

FIG. 11. Aniline + hexane I_{90} data fitting residuals for the $\Delta T_1 = 0.05$ K cross section collected 6 years after sample preparation. (a) Residuals when x_C is fixed at 0.5368, the optimum x_C value from I_{90} data analysis. (b) Residuals when x_C is fixed at 0.5318, the optimum x_C value from coexistence curve analysis.

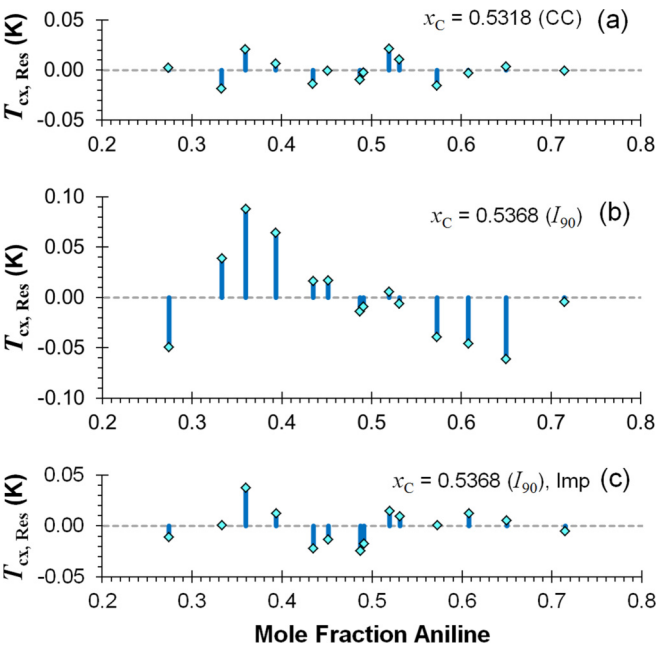

FIG. 12. Initial aniline + hexane coexistence curve fitting residuals using the complete scaling equation truncated at the D_2 term [Eq. (3)]. (a) Residuals when x_C is fixed at 0.5318, with the optimum x_C value from coexistence curve analysis. (b) Residuals when x_C is fixed at 0.5368, with the optimum x_C value from I_{90} data analysis. (c) Residuals when x_C is fixed at 0.5368 and a simple linear impurity correction is included in the complete scaling equation.

TABLE II. Reported methanol + cyclohexane critical composition measurements.

Year reported	Mole fraction methanol	Method of determination	Reference
1930	0.5053	Equal volume criterion	[47]
1943	0.496	Evaluated by the editors of Ref. [35].	[48]
1966	0.489	Evaluated by the editors of Ref. [35].	[49]
1967	0.493	Evaluated by the editors of Ref. [35].	[50]
1970	0.525	Rectilinear diameter analysis	[51]
1977	0.5181 ± 0.0012	Rectilinear diameter analysis	[46]
1978	0.513	Rectilinear diameter analysis	[52]
1983	0.535 ± 0.005	Fit of n_D data to power law; fit of x_C versus water content	[16]
1984	0.539 ± 0.002	Fit of n_D data to power law; fit of x_C versus water content	[36]
1984	0.5219	Meniscus observations	[53]
1985	0.525 ± 0.006	Fit of n_D data to power law	[45]
1986	0.506 ± 0.003	Graphically (unspecified)	[54]
1986	0.5232 ± 0.0006	Meniscus observations	[55]
1986	0.524	Equal volume criterion and rectilinear diameter analysis	[56]
1987	0.5140 ± 0.0006	Fit of T_{cx} data to power law	[57]
1988	0.4986 ± 0.0005	Fit of T_{cx} data to power law	[58]
1988	0.5096 ± 0.0004	Fit of T_{cx} data to power law	[59]
1992	0.508 ± 0.016	T_C was not reported – this is our fit of T_{cx} data to Eq. (3)	[60]
1998	0.5117	Polynomial fit followed by T_{cx} (calculated) fit to power law	[61]
2003	0.4974	Maximum in the coexistence curve	[62]
2006	0.497 ± 0.004	T_C was not reported – this is our fit of T_{cx} data to Eq. (1)	[63]

after the samples were prepared (Fig. 4) yields a $x_{C,Ani}$ of 0.5368 ± 0.0006, a value that is 0.0050 larger. The T_{cx} readings at 6 years were only a few hundredths of a kelvin different from the initial T_{cx} readings, so no significant sample degradation took place in the interim. Furthermore, both $x_{C,Ani}$ values arise from excellent fits to their respective data. Figure 11(a) shows the residuals in a $\Delta T_1 = 0.05$ K slice of the I_{90} surface fit to Eq. (20). The residuals are randomly distributed about zero. The residuals of the coexistence curve fit using truncated complete scaling theory [Eq. (3)] are equally good [Fig. 12(a)]. When each fit is redone with the critical composition fixed to the other method's value of $x_{C,Ani}$, then the residuals exhibit large systematic deviations [Figs. 11(b) and 12(b)]. Therefore the difference between the two $x_{C,Ani}$ values appears to be significant and not a fitting artifact.

We propose that I_{90} data provide the more accurate value for the aniline + hexane critical composition because a simple trace impurity correction brings the coexistence curve data analysis into agreement with the I_{90} data analysis. Binary liquid system critical point temperatures are known to have a linear dependence on impurity concentration [15,16,36–38]. If we hypothesize that component 1 has a trace impurity and component 2 does not, then the resulting impurity-induced shift in coexistence curve temperatures will have a linear dependence on system mole fraction x_1 according to:

$$T_{cx,imp} = T_{cx,0} + a x_1. \tag{22}$$

In Eq. (22), $T_{cx,0}$ is the coexistence curve temperature of the system at composition x_1 with no impurity present in either component, $T_{cx,imp}$ is the coexistence curve temperature when component 1 has an impurity, and a is a constant that depends on the amount and type of impurity present in component 1. Equation (22) may then be combined with Eq. (3) truncated at the D_2 term. Using this revised model, forcing $x_{C,Ani}$ to be 0.5368 actually yields a good fit to the coexistence curve as seen in the resulting residuals [Fig. 12(c)]. The critical temperature changes by 0.3 K with this new fit, which corresponds to a critical composition shift of only 0.0004 according to Eq. (21). From this example, it can be seen how sensitive coexistence curve analysis of the critical composition can be to the presence of trace impurities.

Trace impurities may account for much of the disagreement reported in the literature for liquid-liquid critical compositions, but implementation of I_{90} data analysis has the potential of ameliorating this problem. The technique may be valuable for systematic investigations of impurity effects on x_C and for further evaluation of complete scaling predictions [10,11]. As we will report later, critical amplitudes and constants such as

TABLE III. Reported aniline + hexane critical composition measurements.

Year reported	Mole fraction aniline	Method of determination	Reference
1917	0.499 ± 0.003	T_C was not reported – this is our fit of T_{cx} data to Eq. (1)	[64]
1923	0.566	Not specified	[38]
1958	0.510 ± 0.011	T_C was not reported – this is our fit of T_{cx} data to Eq. (1)	[65]
1967	0.521	Fit of T_{cx} data to power law	[50]
1993	0.504	Interpolated maximum in the coexistence curve	[66]

TABLE IV. Reported isobutyric acid + water critical composition measurements.

Year reported	Mass fraction isobutyric acid	Method of determination	Reference
1965	0.380	Fit of T_{cx} data to power law	[67]
1968	0.388	Fit of T_{cx} data to power law	[68]
1971	0.380	Meniscus observations	[69]
1976	0.389	Rectilinear diameter analysis	[32]
1976	0.383	Equal volume criterion and composition analysis	[70]
1977	0.379	Not specified	[71]
1977	0.3947	Fit of T_{cx} data to power law	[72]
1983	0.384 ± 0.012	Maximum in the coexistence curve	[73]
1988	0.394 ± 0.002	Meniscus observations	[74]
2002	0.3889 ± 0.0008	Fit of T_{cx} data to power law	[33]
2007	0.402 ± 0.004	Fit of T_{cx} data to power law	[75]
2011	0.383 ± 0.002	Equal volume criterion	[76]

the correlation length ξ_0 can also be determined in these experiments. From an applications standpoint, our approach may streamline the process of critical composition determination. For example, rather than creating a set of individual samples, light scattering intensity could be monitored continuously as a function of composition in a titration experiment. This might be especially useful for ternary systems where the critical line or plait points must be identified.

ACKNOWLEDGMENTS

Financial support for the work presented here was provided by the Mary Stuart Rogers Foundation and Willamette University Atkinson Grants.

APPENDIX A: METHANOL + CYCLOHEXANE

An evaluation of methanol + cyclohexane coexistence curve measurements was published in 1994 [35]. The editors found critical compositions for the methanol + cyclohexane system reported in 25 publications, and they recommended a value of 0.515 ± 0.005 mole fraction methanol based on 23 of the publications. However, the editors included 7 publications [15,39–44] where the authors prepared near-critical samples at compositions recommended by earlier work and did not actually make independent measurements of the critical composition. The editors also misidentified the critical compositions reported in three papers [16,45,46].

In our updated survey of the literature, 21 independent measurements of the methanol + cyclohexane critical composition were found (Table II). Each entry in the table lists the year of publication, the value of the critical composition in mole fraction methanol, the uncertainty of the reported value if available, and the method by which the critical composition was determined.

APPENDIX B: ANILINE + HEXANE

Five independent measurements of the aniline + hexane critical composition were found in a search of the literature (Table III). Each entry in the table lists the year of publication, the value of the critical composition in mole fraction aniline, the uncertainty of the reported value if available, and the method by which the critical composition was determined.

APPENDIX C: ISOBUTYRIC ACID + WATER

Twelve independent measurements of the isobutyric acid + water critical composition were found in a search of the literature (Table IV). Each entry in the table lists the year of publication, the value of the critical composition in mass fraction isobutyric acid, the uncertainty of the reported value if available, and the method by which the critical composition was determined.

APPENDIX D: METHANOL + CARBON DISULFIDE

Seven independent measurements of the methanol + carbon disulfide critical composition were found in a search of the literature (Table V). Each entry in the table lists the year of publication, the value of the critical composition in mole

TABLE V. Reported methanol + carbon disulfide critical composition measurements.

Year reported	Mole fraction methanol	Method of determination	Reference
1922	0.296	Interpolated maximum in the coexistence curve	[78]
1923	0.365	Not specified	[38]
1963	0.342	Rectilinear diameter analysis	[79]
1967	0.404	Fit of T_{cx} data to power law	[50]
1970	0.379	Maximum opalescence and equal volume criterion	[77]
	0.365 ± 0.007	Rectilinear diameter and fit of T_{cx} data to power law	
1971	0.364 ± 0.007	Interpolated maximum in the coexistence curve	[80]
1983	0.365 ± 0.007	Equal volume criterion	[81]

fraction methanol, the uncertainty of the reported value if available, and the method by which the critical composition was determined. Viswanathan *et al.* [77] reported one critical composition based on observations of opalescence (0.379) and one based on fitting their coexistence curve data (0.365). We note that the value from their opalescence observations is the closest of all of the literature values to our measured critical composition of 0.3851 [see Fig. 9(c)].

[1] N. V. Plechkova and K. R. Seddon, *Ionic Liquids Uncoiled: Critical Expert Overviews* (Wiley, Hoboken, NJ, 2013).
[2] P. T. Anastas, *Green Solvents: Ionic Liquids* (Wiley-VCH, Weinheim, 2013), Vol. 6.
[3] M. Koel, *Ionic Liquids in Chemical Analysis* (CRC Press, Boca Raton, 2009), Vol. 3.
[4] M. C. Kroon and C. J. Peters, in *Applied Thermodynamics of Fluids*, edited by A. R. H. Goodwin, J. V. Sengers, and C. J. Peters (Royal Society of Chemistry, Cambridge, UK, 2010).
[5] W. Schröer and V. R. Vale, J. Phys.: Condens. Matter **21**, 424119 (2009).
[6] M. Gitterman, *Chemistry Versus Physics: Chemical Reactions Near Critical Points* (World Scientific, Hackensack, NJ, 2010).
[7] A. Kumar, H. R. Krishnamurthy, and E. S. R. Gopal, Phys. Rep. **98**, 57 (1983).
[8] H. Behnejad, J. V. Sengers, and M. A. Anisimov, in *Applied Thermodynamics of Fluids*, edited by A. R. H. Goodwin, J. V. Sengers, and C. J. Peters (Royal Society of Chemistry, Cambridge, UK, 2010).
[9] G. Pérez-Sánchez, P. Losada-Pérez, C. A. Cerdeiriña, J. V. Sengers, and M. A. Anisimov, J. Chem. Phys. **132**, 154502 (2010).
[10] J. Wang, C. A. Cerdeiriña, M. A. Anisimov, and J. V. Sengers, Phys. Rev. E **77**, 031127 (2008).
[11] C. A. Cerdeiriña, M. A. Anisimov, and J. V. Sengers, Chem. Phys. Lett. **424**, 414 (2006).
[12] G. T. Hefter, in *The Experimental Determination of Solubilities*, edited by G. T. Hefter and R. P. T. Tomkins (John Wiley & Sons Ltd., Chichester, UK, 2003).
[13] J. V. Sengers and J. G. Shanks, J. Stat. Phys. **137**, 857 (2009).
[14] K. M. Dean, C. B. Babayco, D. R. B. Sluss, and J. C. Williamson, J. Chem. Phys. **133**, 074506 (2010).
[15] E. Brunner, J. Chem. Thermodyn. **20**, 439 (1988).
[16] J. L. Tveekrem and D. T. Jacobs, Phys. Rev. A **27**, 2773 (1983).
[17] W. I. Goldburg, in *Light Scattering Near Phase Transitions*, edited by H. Z. Cummins and A. P. Levanyuk (North-Holland, Amsterdam, 1983).
[18] B. Chu, Ber. Bunsen-Ges. Phys. Chem. **76**, 202 (1972).
[19] S. Wiegand, M. Kleemeier, J.-M. Schröder, W. Schröer, and H. Weingärtner, Int. J. Thermophys. **15**, 1045 (1994).
[20] R. F. Chang, H. Burstyn, and J. V. Sengers, Phys. Rev. A **19**, 866 (1979).
[21] M. E. Fisher, J. Math. Phys. **5**, 944 (1964).
[22] S. Fusenig and D. Woermann, Ber. Bunsen-Ges. Phys. Chem. **97**, 577 (1993).
[23] C. M. Sorensen and M. D. Semon, Phys. Rev. A **21**, 340 (1980).
[24] B. Chu, F. J. Schoenes, and M. E. Fisher, Phys. Rev. **185**, 219 (1969).
[25] J. Goldsbrough, Science Progress (Oxford) **60**, 281 (1972).
[26] M. Lesemann, A. Martín, L. Belkoura, D. Woermann, and E. Hoinkis, Ber. Bunsen-Ges. Phys. Chem. **101**, 228 (1997).
[27] A. Dega-Dałkowska, Phase Transitions **12**, 337 (1988).
[28] J. Chrapec, S. J. Rzoska, and J. Ziolo, Chem. Phys. **111**, 155 (1987).
[29] G. I. Pozharskaya, N. L. Kasapova, V. P. Skripov, and Y. D. Kolpakov, J. Chem. Thermodyn. **16**, 267 (1984).
[30] J. Osman and C. M. Sorensen, J. Chem. Phys. **73**, 4142 (1980).
[31] K. M. Dean and J. C. Williamson, J. Chem. Eng. Data **56**, 1433 (2011).
[32] S. C. Greer, Phys. Rev. A **14**, 1770 (1976).
[33] A. Toumi, M. Bouanz, and A. Gharbi, Chem. Phys. Lett. **362**, 567 (2002).
[34] D. T. Jacobs, J. Chem. Phys. **91**, 560 (1989).
[35] D. Shaw, A. Skrzecz, J. W. Lorimer, and A. Maczynski, *Solubility Data Series: Alcohols with Hydrocarbons* (Oxford University Press, Oxford, 1994), Vol. 56.
[36] R. H. Cohn and D. T. Jacobs, J. Chem. Phys. **80**, 856 (1984).
[37] R. B. Snyder and C. A. Eckert, J. Chem. Eng. Data **18**, 282 (1973).
[38] C. Drucker, Recl. Trav. Chim. Pays-Bas **42**, 552 (1923).
[39] R. R. Singh and W. A. Van Hook, J. Chem. Thermodyn. **18**, 1021 (1986).
[40] D. Eden, Rev. Sci. Instrum. **53**, 105 (1982).
[41] D. Balasubramanian and P. Mitra, J. Phys. Chem. **83**, 2724 (1979).
[42] B. A. Scheibner, C. M. Sorensen, D. T. Jacobs, R. C. Mockler, and W. J. O'Sullivan, Chem. Phys. **31**, 209 (1978).
[43] J. S. Huang and W. W. Webb, J. Chem. Phys. **50**, 3677 (1969).
[44] C. Warren and W. W. Webb, J. Chem. Phys. **50**, 3694 (1969).
[45] C. Houessou, P. Guenoun, R. Gastaud, F. Perrot, and D. Beysens, Phys. Rev. A **32**, 1818 (1985).
[46] D. T. Jacobs, D. J. Anthony, R. C. Mockler, and W. J. O'Sullivan, Chem. Phys. **20**, 219 (1977).
[47] D. C. Jones and S. Amstell, J. Chem. Soc., 1316 (1930).
[48] E. L. Eckfeldt and W. W. Lucasse, J. Phys. Chem. **47**, 164 (1943).
[49] K. Roth, G. Schneider, and E. U. Franck, Ber. Bunsen-Ges. Phys. Chem. **70**, 5 (1966).
[50] A. N. Campbell and E. M. Kartzmark, Can. J. Chem. **45**, 2433 (1967).
[51] N. V. Kuskova and E. V. Matizen, Sib. Khim. Zh. Izv. Sib. Otd. Akad. Nauk SSR, Ser. Khim Nauk, 142 (1970).
[52] F. Becker, M. Kiefer, P. Rhensius, A. Spoerner, and A. Steiger, Z. Phys. Chem. (Munich) **112**, 139 (1978).
[53] R. B. Kopelman, R. W. Gammon, and M. R. Moldover, Phys. Rev. A **29**, 2048 (1984).
[54] G. Hradetzky and H.-J. Bittrich, Int. DATA Ser., Sel. Data Mixtures, Ser. A, 218 (1986).
[55] D. T. Jacobs, Phys. Rev. A **33**, 2605 (1986).
[56] W. Schön, R. Wiechers, and D. Woermann, J. Chem. Phys. **85**, 2922 (1986).
[57] R. R. Singh and W. A. Van Hook, J. Chem. Phys. **87**, 6097 (1987).
[58] A. G. Aizpiri, R. G. Rubio, and M. Diaz Pena, J. Chem. Phys. **88**, 1934 (1988).

[59] M. B. Ewing, K. A. Johnson, and M. L. McGlashan, J. Chem. Thermodyn. **20**, 49 (1988).
[60] M. Kato, T. Muramatsu, H. Ueda, M. Yamaguchi, and T. Ozawa, Sekiyu Gakkaishi **35**, 312 (1992).
[61] H. Marhold, P. Waldner, and H. Gamsjäger, Thermochim. Acta **321**, 127 (1998).
[62] H. Matsuda, K. Ochi, and K. Kojima, J. Chem. Eng. Data **48**, 184 (2003).
[63] A. Trejo, P. Yañez, and R. Eustaquio-Rincón, J. Chem. Eng. Data **51**, 1070 (2006).
[64] D. B. Keyes and J. H. Hildebrand, J. Am. Chem. Soc. **39**, 2126 (1917).
[65] K. Zięborak, Bulletin de l'Académie Polonaise des Sciences. Série des sciences chimiques, géologiques, et géographiques **6**, 443 (1958).
[66] K. Ochi, M. Momose, K. Kojima, and B. C.-Y. Lu, Can. J. Chem. Eng. **71**, 982 (1993).
[67] D. Woermann and W. Sarholz, Ber. Bunsen-Ges. Phys. Chem. **69**, 319 (1965).
[68] B. Chu, F. J. Schoenes, and W. P. Kao, J. Am. Chem. Soc. **90**, 3042 (1968).
[69] J. C. Allegra, A. Stein, and G. F. Allen, J. Chem. Phys. **55**, 1716 (1971).
[70] G. Morrison and C. M. Knobler, J. Chem. Phys. **65**, 5507 (1976).
[71] H. Klein and D. Woermann, Ber. Bunsen-Ges. Phys. Chem. **81**, 1081 (1977).
[72] T. S. Venkataraman and L. M. Narducci, J. Phys. C: Sol. State **10**, 2849 (1977).
[73] D. V. Fenby, J. R. Khurma, Z. S. Kooner, and R. F. Smith, Aust. J. Chem. **36**, 215 (1983).
[74] R. F. Berg and M. R. Moldover, J. Chem. Phys. **89**, 3694 (1988).
[75] A. Siporska, A. Makowska, and J. Szydłowski, J. Phys. Chem. B **111**, 11632 (2007).
[76] P. Madhusudhana Reddy, P. Venkatesu, and H. B. Bohidar, J. Phys. Chem. B **115**, 12065 (2011).
[77] B. Viswanathan, R. D. Gambhir, and E. S. R. Gopal, J. Chem. Phys. **53**, 4405 (1970).
[78] E. C. McKelvy and D. H. Simpson, J. Am. Chem. Soc. **44**, 105 (1922).
[79] P. Franzosini, Z. Naturforsch. A **18**, 224 (1963).
[80] R. D. Gambhir, B. Viswanathan, and E. S. R. Gopal, Indian J. Pure Ap. Phy. **9**, 787 (1971).
[81] U. Oswald and D. Woermann, Ber. Bunsen-Ges. Phys. Chem. **87**, 654 (1983).